PHILOSOPHICAL TRANSACTIONS A

rsta.royalsocietypublishing.org

Review

Cite this article: Wohlgenannt M, Flatté ME, Harmon NJ, Wang F, Kent AD, Macià F. 2015 Singlet-to-triplet interconversion using hyperfine as well as ferromagnetic fringe fields. *Phil. Trans. R. Soc. A* **373**: 20140326. http://dx.doi.org/10.1098/rsta.2014.0326

Accepted: 1 April 2015

One contribution of 11 to a discussion meeting issue 'Organic semiconductor spintronics: utilizing triplet excitons in organic electronics'.

Subject Areas:
spintronics, solid-state physics, nanotechnology

Keywords:
organic spintronics, spin-chemistry, magnetic-field effect, magnetoresistance

Author for correspondence:
M. Wohlgenannt
e-mail: markus-wohlgenannt@uiowa.edu

Singlet-to-triplet interconversion using hyperfine as well as ferromagnetic fringe fields

M. Wohlgenannt[1], M. E. Flatté[1], N. J. Harmon[1], F. Wang[1], A. D. Kent[2] and F. Macià[2]

[1]Department of Physics and Astronomy and Optical Science and Technology Center, University of Iowa, Iowa City, IA 52242, USA
[2]Department of Physics, New York University, 4 Washington Place, New York, NY 10003, USA

Until recently the important role that spin-physics ('spintronics') plays in organic light-emitting devices and photovoltaic cells was not sufficiently recognized. This attitude has begun to change. We review our recent work that shows that spatially rapidly varying local magnetic fields that may be present in the organic layer dramatically affect electronic transport properties and electroluminescence efficiency. Competition between spin-dynamics due to these spatially varying fields and an applied, spatially homogeneous magnetic field leads to large magnetoresistance, even at room temperature where the thermodynamic influences of the resulting nuclear and electronic Zeeman splittings are negligible. Spatially rapidly varying local magnetic fields are naturally present in many organic materials in the form of nuclear hyperfine fields, but we will also review a second method of controlling the electrical conductivity/electroluminescence, using the spatially varying magnetic fringe fields of a magnetically unsaturated ferromagnet. Fringe-field magnetoresistance has a magnitude of several per cent and is hysteretic and anisotropic. This new method of control is sensitive to even remanent magnetic states, leading to different conductivity/electroluminescence values in the absence of an applied field. We briefly review a model based on fringe-field-induced polaron-pair spin-dynamics that successfully describes several key features of the experimental fringe-field magnetoresistance and magnetoelectroluminescence.

THE ROYAL SOCIETY PUBLISHING

1. Introduction

Spintronics is the science and technology that deals with controlling and using the electron spin degree of freedom through a variety of phenomena. Most spintronic devices rely on a change in the relative magnetizations of two magnetic electrodes to control the flow of electronic current through a non-magnetic material [1–3], such as by spin-selective scattering (as in current-in-plane giant magnetoresistance) [4,5] or by spin-injection (as in current-perpendicular-to-plane giant magnetoresistance) [6]. If the two ferromagnetic electrodes are chosen to exhibit two distinct switching fields, the device can be switched between a parallel and antiparallel magnetization configuration using an applied magnetic field, B. A current-perpendicular-to-plane giant magnetoresistive device is often referred to as a spin-valve. If a dielectric layer replaces the metallic spacer layer between the two ferromagnetic layers, it forms a magnetic tunnel junction, and the corresponding effect is called tunnelling magnetoresistance [7,8].

Using semiconductors as spacer layers (instead of metals or dielectrics) is a third and particularly attractive option because of the possibility of implementing spintronic logic devices. However, spin-injection into semiconductors continues to pose challenges, in part because of the conductivity mismatch problem [9]. The search for new materials systems is therefore ongoing. In particular, there has been increasing interest in using organic semiconductors for spintronics. The use of organic semiconductors is motivated, in part, by their long spin relaxation times [10,11]. The first demonstration of an organic spintronic device employed a planar structure of $La_{2/3}Sr_{1/3}MnO_3$ (LSMO) electrodes separated by an ≈ 100 nm long channel of α-sexithiophene [12]. The first vertical organic spin-valve device, which used LSMO and Co as the ferromagnetic layers, was demonstrated by Xiong *et al.* [13].

2. Hyperfine-induced magnetoresistance

In addition to the organic spin-valve effect, whose underlying physics largely mirrors the spin-valve effect known from inorganic materials, there occur a variety of spin-dependent processes in organic semiconductor devices. A particular example is the large, room-temperature magnetoresistive effect known as organic magnetoresistance (OMAR) [14–17]. Contrary to the spin-valve effect, OMAR devices do not use magnetic electrodes; rather, the effect occurs in regular organic light-emitting diodes (OLEDs). The physics of the effect is therefore completely different from that of spin-valves, and it is unrelated to spin-polarized injection. Figure 1*a* shows a typical OMAR trace measured in OLED devices based on a variety of organic semiconductor materials. The magnetoconductivity (or magnetoresistance) is defined here to be the difference between the conductivity measured at finite magnetic field and that measured at zero magnetic field, normalized by the conductivity (or resistance) at zero magnetic field. The magnitude of the effect is typically 10%. Experimentally, it has been established that OMAR is approximately independent of the magnetic-field direction [15,18] and that in most materials it obeys empirical laws given by either a Lorentzian $\Delta I(B)/I \propto B^2/(B^2 + B_0^2)$ or the non-Lorentzian lineshape $\Delta I(B)/I \propto B^2/(|B| + B_0)^2$, depending on the material, for the change in the current I with magnetic field B, where $B_0 \approx 5$ mT [18].

It is now believed that OMAR is akin to what are called magnetic-field effects in spin-chemistry [20]. Spin-chemistry studies spin-selective reactions between spin-carrying, or paramagnetic, entities. In OLED devices, paramagnetic entities are present in the form of electrons, holes and triplet excitons. Furthermore, as in spin-chemistry, an important role is thought to be played by the hyperfine interaction, i.e. the coupling of the electronic and nuclear spins. The paramagnetic entity experiences a local hyperfine field (B_{hf}) of the order of 1 mT, originating mainly from the hydrogen nuclei. B_{hf} varies randomly from site to site and causes mixing between the singlet and triplet spin states of a pair of paramagnetic entities on neighbouring molecules, as will be explained in more detail below. An externally applied field exceeding the hyperfine field suppresses this spin mixing and therefore changes the reaction rate between the entities. The relevance of hyperfine fields for OMAR has been demonstrated by targeted

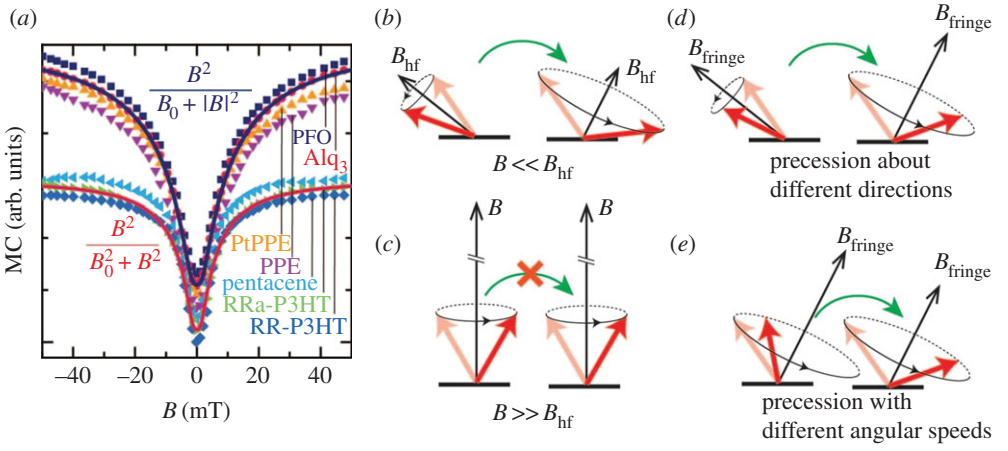

Figure 1. (*a*) Typical OMAR traces (magnetoconductance MC versus applied magnetic field *B*) for a wide variety of polymers (PFO, PtPPE, PPE, RRa-PsHT and RR-P3Ht) and small molecule (Alq_3 and pentacene) devices, all showing either a Lorentzian ($B^2/(B_0^2 + B^2)$) or a specific non-Lorentzian ($B^2/(B_0 + |B|)^2$) dependence. For details, see [18]. The magnitude of the effect is typically 10%. (*b–e*) Pauli spin blocking in the formation of a singlet (S) bipolaron, after arrival of two charge carriers at neighbouring molecules in a triplet (T) spin configuration (light coloured red arrows). (*b*) When $B \ll B_{hf}$, the two spins precess about different hyperfine fields, mixing in S character, and bipolaron formation is possible. (*c*) When $B \gg B_{hf}$, the two spins precess about the same field *B* and remain in a T configuration (dark coloured red arrows); bipolaron formation remains blocked. In the presence of fringe fields, lifting of the blockade can also take place because (*d*) they have different directions or (*e*) different magnitudes at the two molecules. PFO, polyfluorene; PtPPE, platinum-containing polyphenylene-ethynelene; PPE, polyphenylene-ethynelene; RRa-P3HT, regio-random polythiophene; RR-P3Ht, regio-regular polythiophene; Alq_3, 8-tris-hydroxyquinoline aluminium; B_0, characteristic magnetic-field scale; B_{hf}, hyperfine magnetic-field strength; B_{fringe}, field of a ferromagnetic layer. (Adapted from [19].) (Online version in colour.)

experiments comparing OMAR in ordinary and deuterated polymer devices [21]. However, what paramagnetic entities are involved and how their spin-dependent interactions yield the experimentally observed OMAR effect is still debated. Several mechanisms have been suggested. For the purpose of illustrating the basic mechanism, we now discuss in some more detail one of these mechanisms, the bipolaron mechanism [22]. In figure 1*b*,*c*, we consider two neighbouring molecules. We suppose that two charge carriers of like charge have arrived at these molecules in a triplet *T* configuration (e.g. the spins of the two charges are aligned). In that case, a carrier on one of the molecules cannot hop to the other molecule in the same orbital as the other carrier because of the Pauli exclusion principle. In other words, the resulting Pauli spin-blockade prevents 'bipolaron' formation. If, in addition, one of the two charges is immobile ('trapped'), then this spin-blockade shuts off any electrical conduction through this molecule, and the device current is suppressed. However, if $B \ll B_{hf}$, precession of the spins about the different hyperfine fields at the two molecules mixes in singlet S character, lifting the blockade and allowing bipolaron formation, resulting in current flow (figure 1*b*). On the other hand, if $B \gg B_{hf}$, both spins process around the same field, and the carriers remain in a T configuration, preventing lifting of the blockade (figure 1*c*). Apart from this bipolaron mechanism, two other kinds of mechanisms have been put forward as possible explanations for OMAR, which differ in the paramagnetic entities involved. (i) The electron–hole pair model [15,16] in which the spin-selective reaction between oppositely charged polarons to form an exciton (recombination) is of central importance. (ii) The triplet exciton–polaron model [23], which is based on the trapping of charges by triplet excitons.

The magnitude of the effect is typically 10%. However, a recent report [24] has achieved an exceptionally large (more than 2000%), room-temperature OMAR effect in one-dimensional, non-magnetic systems formed by molecular wires embedded in a zeolite host crystal. This

ultrahigh magnetoresistance effect is ascribed to spin-blockade in one-dimensional electron transport. This enhancement in one-dimensional systems is easy to understand: whereas carriers hopping through a three-dimensional sample can easily avoid each other and/or circumvent any spin-blocked sites, this is not possible in a one-dimensional motion. The generic nature of this enhancement offers very good perspectives to exploit the effect in a wide range of low-dimensional systems.

OMAR is only one example of spin-dependent processes that occur in organic semiconductor devices. Recently, it has been realized that spin-dependent processes crucially factor into the efficiency of OLEDs and organic photovoltaic cells. We will briefly review two such processes. (i) Singlet exciton fission transforms a molecular singlet excited state into two triplet states, each with half the energy of the original singlet. In solar cells, it could potentially double the photocurrent from high-energy photons. Congreve *et al.* [25] recently demonstrated organic solar cells that exploit singlet exciton fission in pentacene to generate more than one electron per incident photon in a portion of the visible spectrum. Using a fullerene acceptor, a poly(3-hexylthiophene) exciton confinement layer, and a conventional optical trapping scheme, they achieved a peak external quantum efficiency of $(109 \pm 1)\%$ at a wavelength of 670 nm for a 15-nm-thick pentacene film. The corresponding internal quantum efficiency is $(160 \pm 10)\%$. They performed an analysis of the magnetic-field effect on photocurrent that suggests that the triplet yield approaches 200% for pentacene films thicker than 5 nm. (ii) Adachi and co-workers [26] recently demonstrated materials that possess a very small energy gap between its singlet and triplet excited states. This makes it possible to efficiently up-convert triplet states into a singlet state. The effect is called thermally activated delayed fluorescence.

3. Fringe-field-induced magnetoresistance and magnetoelectroluminescence

Before we turn to the next topic, let us briefly review the key points underlying the OMAR effect. Two types of magnetic fields play a central role: (i) the applied magnetic field, which is spatially homogeneous and has the tendency to lock the spin-state of a paramagnetic pair, and (ii) the hyperfine magnetic field, which is spatially inhomogeneous and has the tendency to mix singlet and triplet spin-states. The measured magnetoconductance (MC) results from a competition between the two via spin-selective scattering events: the low-field conductivity is determined by spin-selective scattering events where the spin-state is free, whereas the high-field conductivity is determined by spin-selective scattering events where the spin-state is constrained.

Typically, the source of the spin-mixing, inhomogeneous field is the nuclear hyperfine field, which is random and spatially uncorrelated (i.e. it varies randomly from one molecule to the next). More recently it was recognized that spin-mixing can also occur even if the inhomogeneous field is spatially correlated over many molecular spacings. All that is required is that there exist significant gradients in local magnetic-field strength [27]. Figure 1*e* illustrates the basics of the effect. If a local field gradient exists, the two spins located on the two molecules will precess with a different rate. As a result, a phase difference between the two spinors develops with time, and singlet–triplet interconversion can occur, because the singlet spinor differs from the triplet, $m = 0$ spinor only by a relative phase.

Therefore, a critical ingredient for OMAR devices is a spatially varying magnetic-field landscape, which is usually provided by the molecular hyperfine fields. However, it can be beneficial to instead rely on an externally supplied magnetic-field landscape. In that case, the response function of the OMAR traces can be engineered to match a desired application. Whereas OMAR sensors based on hyperfine magnetic fields are sensitive only in the 1–10 mT range, are non-hysteretic (i.e. they cannot sense the sign of the applied magnetic field) and essentially isotropic (i.e. they cannot sense the field direction), OMAR sensors based on an externally supplied field-landscape may be sensitive to different field-magnitude ranges, be hysteretic and anisotropic. Such 'extrinsic' OMAR devices were recently demonstrated [28] using fringe fields emitted from a nearby ferromagnetic film as the source of the magnetic-field landscape.

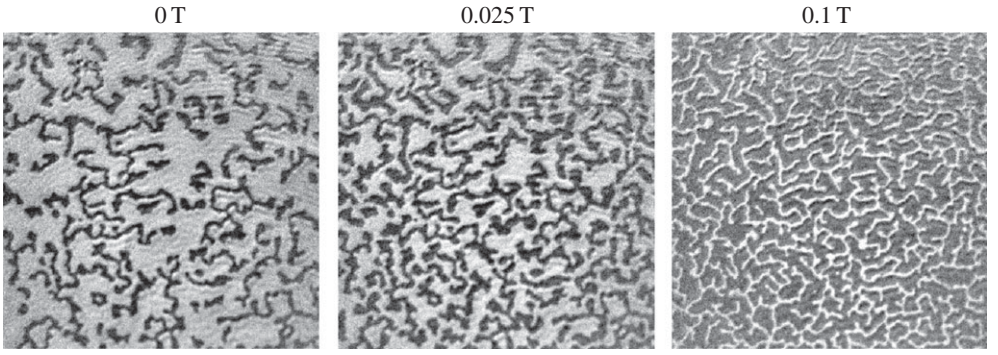

Figure 2. Domain structure of the magnetic film used in fringe-field organic magnetoresistive devices as measured by X-ray microscopy for several different applied magnetic fields. The images shown cover an area of $5 \times 5\,\mu$m. The fields are applied in a direction perpendicular to the magnetic film plane. For details, see [28]. (Adapted from [31].)

Magnetic fringe fields induced by a ferromagnet are mainly determined by the magnetic domain structure. For a film with magnetic anisotropy, the domain structure is highly anisotropic and hysteretic and it can be controlled by engineering the magnetic media [29,30]. The strength and the spatial-correlation length of fringe fields from a ferromagnet also depend sensitively on the distance from the ferromanget. Wang *et al.* [28] used a film of alternating Co and Pt layers with perpendicular magnetic anisotropy (PMA) as the source of magnetic fringe fields. This magnetic film with PMA can be magnetized (i.e. a state without magnetic domains) by large perpendicular magnetic fields and demagnetized (magnetic domains reappear) by large in-plane magnetic fields. Note that it is a characteristic of perfectly flat, saturated, perpendicularly magnetized films that they produce no fringe fields above the films far from the edges; fringe fields above the film originate from the presence of domains in unsaturated states. Transmission X-ray microscopy based on the X-ray magnetic circular dichroism (XMCD) effect is used to determine the microscopic magnetic domain structure of the magnetic film [28]. Several example images are shown in figure 2, which show the magnetic film transitioning from a state with mostly down domains (light grey) to mostly up domains (dark domains) as the applied magnetic field is increased as part of a magnetization loop. XMCD images are used to determine the magnetic fringe fields at different distances above the ferromagnetic layer. The fringe-field strength anywhere in space can be calculated from the domain geometry [28].

'Fringe-field OMAR' devices consist of regular OMAR devices fabricated directly on top of a ferromagnetic film consisting of a Co–Pt multi-layer (figure 3) [27]. The magnetic-field effects can be studied by measuring both the MC and the magnetoelectroluminescence (MEL), i.e. the dependence of the electroluminescence (EL) on the magnetic field. To study the dependence of the device response on the distance separating the OMAR device and fringe-field source, a conducting polymer spacer layer of variable thickness was inserted between the OMAR device and the ferromagnetic film. In the presence of a large magnetic field out of the film plane, the Co–Pt films are uniformly magnetized with all the spins pointing opposite to the direction of the applied field. At lower fields, the films form magnetic domains—some regions with spins pointing up and others with spins pointing down—to lower the magnetostatic energy. These magnetic domains create strong, spatially varying fringe fields close to the surface of the Co–Pt films, which penetrate the OMAR/OLED device. Figure 3*b* shows a typical MC and MEL trace, and figure 3*c* the current–voltage (IV) and EL curves, for an organic device without a magnetic film and whose MC/MEL is therefore caused by the random hyperfine fields, as described above. This device serves as a reference when, later on, we will discuss fringe-field-induced MC/MEL. It is seen that the hyperfine-induced MC and MEL responses have a magnitude of $\approx$5% and $\approx$10%, respectively, in poly[2-methoxy-5-(2-ethylhexyloxy)-1,4-phenylenevinylene] (MEHPPV) devices.

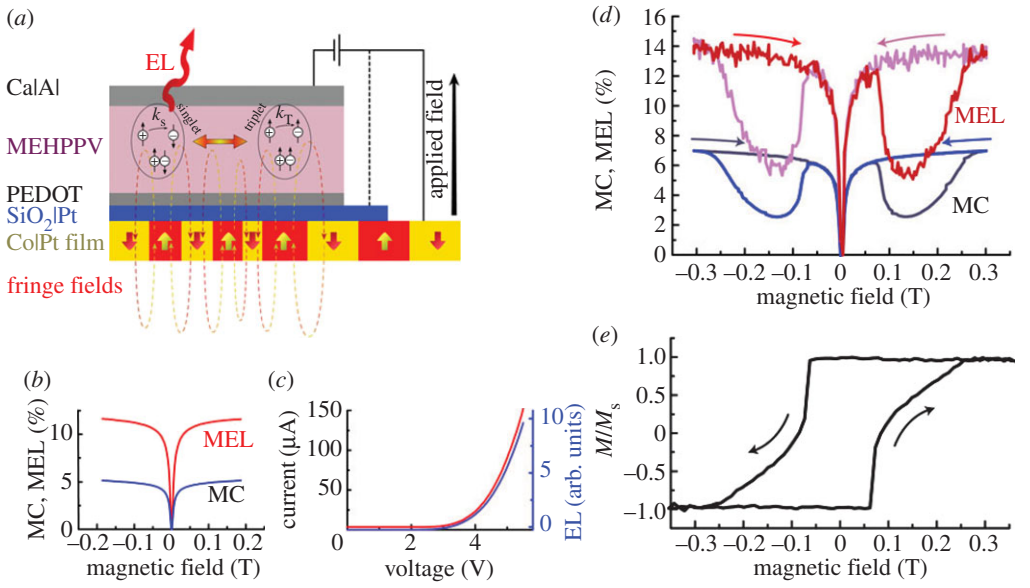

Figure 3. (*a*) Schematic of the device structure used for fringe-field MC and MEL measurements. The device consists of a standard OMAR/OLED device fabricated on top of a ferromagnetic film, which need not be in electrical contact with the organic device. A SiO_2 layer was used in some devices to electrically isolate the magnetic film from the organic device. The electroluminescence (EL) is collected through the semitransparent top contact. (*b*) MC and MEL responses to an external magnetic field of a reference OMAR/OLED device without the magnetic film and (*c*) IV and EL versus voltage for the reference device. (*d*) MC and MEL responses of the complete organic fringe-field device. (*e*) Magnetization *M* relative to the saturation magnitization MS of the ferromagnetic film as obtained by the magneto-optic Kerr effect (MOKE). All data are for room temperature. (Adapted from [27].) (Online version in colour.)

The effects essentially saturate for applied fields in excess of 0.1 T, are non-hysteretic and have a full width at half maximum of ≈20 mT. The effects are also independent of the direction of the applied magnetic field, and nearly independent of the MEHPPV layer thickness. In the present work, we have chosen to work with a thin MEHPPV layer (55 nm) such that the distance from the ferromagnetic film does not vary much between different locations in the MEHPPV film.

Now we turn our attention to the MC/MEL responses of the fringe-field OMAR devices, and the correlation between these effects and the film magnetization, *M*. Figure 3*d* shows the measured MC and MEL curves, and figure 3*e* shows the magnetization loop measured by the magneto-optic Kerr effect (MOKE). In these measurements, the magnetic field is applied perpendicularly to the device plane and is swept smoothly from large negative to large positive fields and back (black lines). It is seen that the magnetization response is hysteretic and that *M* assumes its saturation value for fields larger than ≈0.25 T in magnitude. *M* is unsaturated between roughly 0.05 and 0.25 T. The MC/MEL curves outside the unsaturated magnetization regime clearly mirror the data in non-magnetic devices (figure 3*b*) and are explained by the 'normal' hyperfine OMAR effect. In the unsaturated region, the data curves develop characteristic 'ears'. In addition to a magnetoconductive response, the fringe-field effects lead to a sizable room-temperature MEL response, of up to 6% at room temperature for the present device. This can be comparable to MEL effects that occur only at low temperature, such as those recently reported in spin-valves [32].

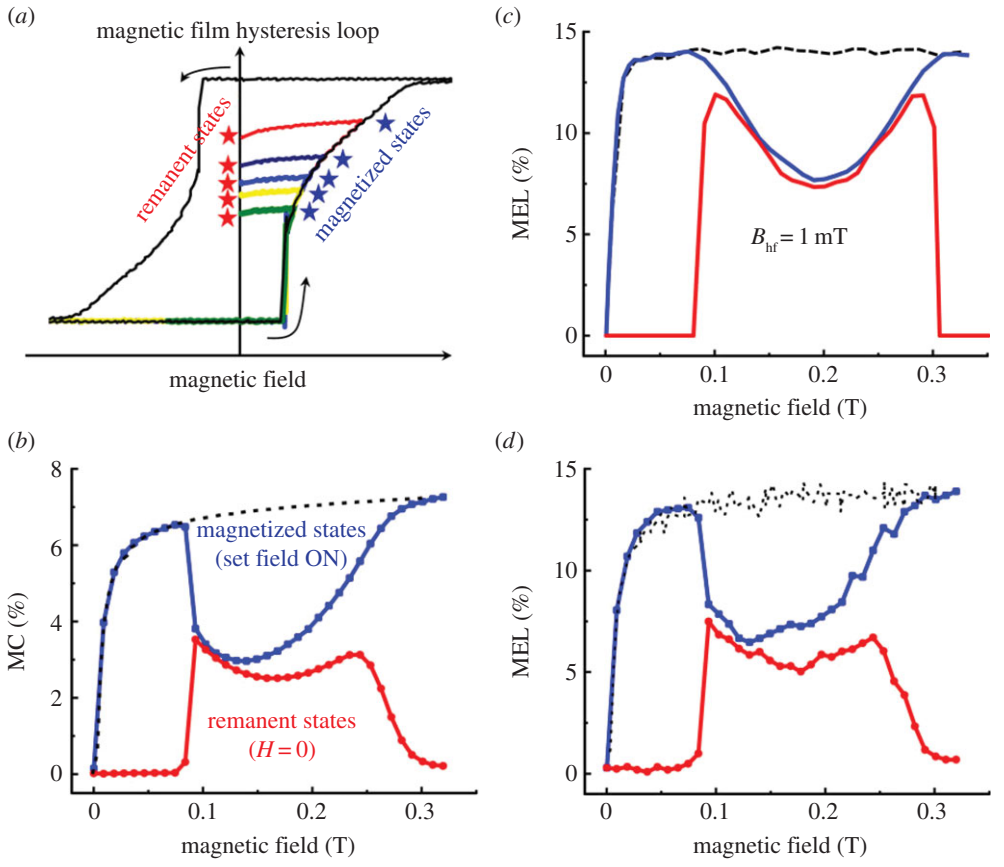

Figure 4. In these measurements, the applied magnetic field plays an auxiliary role and is used to write ('set') a particular remanent magnetic state, corresponding to a particular domain configuration and particular fringe-field pattern, and to erase ('reset') this configuration by replacing it with a saturated state without domains. This saturated state without domains is also used as the reference state for the MC and MEL percentage responses. Referring to the magnetization loop of an example magnetic film, panel (*a*) shows the procedure to set and reset different remanent states. The set field (blue star) is used to select a magnetic state. As the set field is being removed, the film remains in essentially the same state as evidenced by the only small amount of relaxation in magnetization between the write state (blue star) and the remanent state (red star). (*b*) Conductance and (*d*) EL referenced to a fully saturated state measured in different magnetic states of the ferromagnetic film versus the set field strength (red curve). For comparison, the conductance and EL value measured while the set field is still on is also shown (blue curve). Grey dashed curves correspond to measured values of conductance (*b*) and EL (*d*) at the set field when the magnetic film is saturated. (*c*) Theoretical calculation following text, using switching fields from figure 1*e*, to be compared with (*d*). Grey dashed curve is the calculation with the fringe fields absent. (Adapted from [27].) (Online version in colour.)

(a) Control of electroluminescence with remanent fields

Magnetic domains can be present at zero applied field in magnetic films. In the devices reported by Macia *et al.* [27], such remanent states are prepared by applying a perpendicular field close to the film's coercive field and then removing it (figure 4*a*). With this method, one has access to remanent magnetization states ranging from negative to positive saturation. At zero applied field, we observed how remanent fringe fields increase the conductance of the organic layer MEHPPV, suppressing OMAR. Figure 4*b*,*d* shows MC and MEL of a MEHPPV fringe-field device both in the presence of and at zero magnetic field. The blue line depicts the measured values in the presence of a magnetic field, whereas the red lines trace the values measured after removing the applied field (a sketch of the measuring sequence is shown in figure 4*a*). First, the sample is saturated with

a large negative field, then a positive field value from 0 to 0.3 T is set and the device conductivity is measured (blue points). Finally, the applied field is removed and the device conductivity is measured once again (red points). Figure 4 shows that the EL increases up to 6% for remanent magnetic domain states of the ferromagnetic layer. In contrast to fringe fields from the same domain configuration in an applied magnetic field (near the coercive field), the MEL increases rather than decreases.

(b) Theory of magnetic fringe-field effects on magnetoconductance and magnetoelectroluminescence

A successful theory of the fringe-field MEL has been developed [27]. In this theory, a two-site model where an electron and hole (a polaron pair) occupy two nearby sites is considered. The spin configuration of the polaron pair undergoes transitions due to the different magnetic interactions present; these interactions consist of Zeeman-type interactions between the two spins and their respective local fringe/hyperfine field. The polaron pairs recombine into excitons at different rates, k_S and k_T, depending on the pair's spin, as the singlet and triplet states have different energies and wave functions. Once an exciton is formed, the large exchange energy precludes any further spin evolution. In the absence of large spin–orbit interactions, spin-selection rules dictate that exciton recombination (i.e. photon emission) occurs only from the singlet exciton state. Therefore, the MEL can be calculated from the singlet fraction of excitons. To calculate the MEL, the stochastic Liouville equation for the polaron pair spin-density matrix is employed. To proceed with the calculation, one must have knowledge of the fringe fields present in the organic layer. As was described above, elementary magnetostatics can be used to calculate fringe fields from XMCD images of the magnetic domains (figure 2). The results of this theory and model are shown in figure 4*c*. The agreement between model and experiment is very good.

4. Conclusion

Recently, the OLED and photovoltaics community has begun to realize that spintronics plays a crucial role in these devices. Examples for this include singlet fission processes that enhance the efficiency of organic photovoltaic cells, and thermally assisted delayed fluorescence, which pushes the internal EL quantum efficiency beyond the naive 25% spin-statistical limit. OMAR and MEL allows the device current and light-emission intensity to be controlled using an applied magnetic field, or even using a remanent magnetic field of a nearby ferromagnetic film. We showed that OMAR and MEL arises from a competition between spin-dynamics due to spatially varying fields and an applied, spatially homogeneous magnetic field. The effects exist even at room temperature where the thermodynamic influences of the resulting nuclear and electronic Zeeman splittings are negligible. Spatially rapidly varying local magnetic fields are naturally present in many organic materials in the form of nuclear hyperfine fields, but we demonstrated a second method where the magnetic-field landscape was provided from outside the organic layer, using the spatially varying magnetic fringe fields of a magnetically unsaturated ferromagnet. Typical OMAR and MEL effects have a relative magnitude of about 10%, but recent work in molecular wires has shown that this can be enhanced to a near perfect 100% effect.

Acknowledgements. We acknowledge useful conversations with P. Fischer, M.-Y. Im and P. A. Bobbert.

Funding statement. All authors were supported by ARO MURI grant no. W911NF-08-1-0317. F.M. is grateful for additional support from EU, MC-IOF 253214.

Authors' contributions. M.W. participated in the conception of the study, supervised the fabrication and measurements of the organic devices, and drafted the manuscript. M.E.F. participated in the conception of the study, supervised the formulation of the fringe-field gradient model and contributed to the manuscript. N.J.H. performed the fringe-field gradient model calculations. F.W. performed the device fabrication and measurements of the fringe-field organic devices. A.D.K. participated in the conception of the study,

supervised the magnetic film deposition and contributed to the manuscript. F.M. performed the deposition and patterning of the magnetic films used in the fringe-field devices.

Conflict of interests. We hereby declare that none of the authors have any competing interests.

References

1. Wolf SA, Awschalom DD, Buhrman RA, Daughton JM, von Molnar S, Roukes ML, Chtchelkanova AY, Treger DM. 2001 Spintronics: a spin-based electronics vision for the future. *Science* **294**, 1488–1495. (doi:10.1126/science.1065389)
2. Awschalom DD, Flatté ME. 2007 Challenges for semiconductor spintronics. *Nat. Phys.* **3**, 153–159. (doi:10.1038/nphys551)
3. Flatté ME. 2007 Spintronics. *IEEE Trans. Electron Devices* **54**, 907–920. (doi:10.1109/TED.2007.894376)
4. Baibich MN, Broto JM, Fert A, Vandau FN, Petroff F, Eitenne P, Creuzet G, Friederich A, Chazelas J. 1988 Giant magnetoresistance of (001)Fe/(001) Cr magnetic superlattices. *Phys. Rev. Lett.* **61**, 2472–2475. (doi:10.1103/PhysRevLett.61.2472)
5. Binasch G, Grunberg P, Saurenbach F, Zinn W. 1989 Enhanced magnetoresistance in layered magnetic-structures with antiferromagnetic interlayer exchange. *Phys. Rev. B* **39**, 4828–4830. (doi:10.1103/PhysRevB.39.4828)
6. Johnson M, Silsbee RH. 1988 Spin-injection experiment. *Phys. Rev. B* **37**, 5326–5335. (doi:10.1103/PhysRevB.37.5326)
7. Julliere M. 1975 Tunneling between ferromagnetic-films. *Phys. Lett. A* **54**, 225–226. (doi:10.1016/0375-9601(75)90174-7)
8. Moodera JS, Kinder LR, Wong TM, Meservey R. 1995 Large magnetoresistance at room-temperature in ferromagnetic thin-film tunnel-junctions. *Phys. Rev. Lett.* **74**, 3273–3276. (doi:10.1103/PhysRevLett.74.3273)
9. Schmidt G, Ferrand D, Molenkamp LW, Filip AT, van Wees BJ. 2000 Fundamental obstacle for electrical spin injection from a ferromagnetic metal into a diffusive semiconductor. *Phys. Rev. B* **62**, R4790–R4793. (doi:10.1103/PhysRevB.62.R4790)
10. Naber WJM, Faez S, van der Wiel WG. 2007 Organic spintronics. *J. Phys. D Appl. Phys.* **40**, R205–R228. (doi:10.1088/0022-3727/40/12/R01)
11. Dediu VA, Hueso LE, Bergenti I, Taliani C. 2009 Spin routes in organic semiconductors. *Nat. Mater.* **8**, 707–716. (doi:10.1038/nmat2510)
12. Dediu V, Murgia M, Matacotta FC, Taliani C, Barbanera S. 2002 Room temperature spin polarized injection in organic semiconductor. *Solid State Commun.* **122**, 181–184. (doi:10.1016/S0038-1098(02)00090-X)
13. Xiong ZH, Wu D, Vardeny ZV, Shi J. 2004 Giant magnetoresistance in organic spin-valves. *Nature* **427**, 821–824. (doi:10.1038/nature02325)
14. Francis TL, Mermer O, Veeraraghavan G, Wohlgenannt M. 2004 Large magnetoresistance at room temperature in semiconducting polymer sandwich devices. *N. J. Phys.* **6**, 185. (doi:10.1088/1367-2630/6/1/185)
15. Prigodin VN, Bergeson JD, Lincoln DM, Epstein AJ. 2006 Anomalous room temperature magnetoresistance in organic semiconductors. *Synth. Met.* **156**, 757–761. (doi:10.1016/j.synthmet.2006.04.010)
16. Hu B, Wu Y. 2007 Tuning magnetoresistance between positive and negative values in organic semiconductors. *Nat. Mater.* **6**, 985–991. (doi:10.1038/nmat2034)
17. Bloom FL, Wagemans W, Kemerink M, Koopmans B. 2007 Separating positive and negative magnetoresistance in organic semiconductor devices. *Phys. Rev. Lett.* **99**, 257201. (doi:10.1103/PhysRevLett.99.257201)
18. Mermer Ö, Veeraraghavan G, Francis TL, Sheng Y, Nguyen DT, Wohlgenannt M, Köhler A, Al-Suti MK, Khan MS. 2005 Large magnetoresistance in nonmagnetic pi-conjugated semiconductor thin film devices. *Phys. Rev. B* **72**, 205202. (doi:10.1103/PhysRevB.72.205202)
19. Wohlgenannt M, Bobbert PA, Koopmans B. 2014 Intrinsic magnetic field effects in organic semiconductors. *MRS Bull.* **39**, 590–595. (doi:10.1557/mrs.2014.132)
20. Schulten K. 1982 Magnetic-field effects in chemistry and biology. *Fertkorperprobleme-Adv. Solid State Phys.* **22**, 61–83. (doi:10.1007/BFb0107935)
21. Nguyen TD, Hukic-Markosian G, Wang FJ, Wojcik L, Li XG, Ehrenfreund E. 2010 Isotope effect in spin response of pi-conjugated polymer films and devices. *Nat. Mater.* **9**, 345–352. (doi:10.1038/nmat2633)

22. Bobbert PA, Nguyen TD, van Oost FWA, Koopmans B, Wohlgenannt M. 2007 Bipolaron mechanism for organic magnetoresistance. *Phys. Rev. Lett.* **99**, 216801. (doi:10.1103/PhysRevLett.99.216801)
23. Desai P, Shakya P, Kreouzis T, Gillin WP, Morley NA, Gibbs MRJ. 2007 Magnetoresistance and efficiency measurements of Alq(3)-based OLEDs. *Phys. Rev. B* **75**, 094423. (doi:10.1103/PhysRevB.75.094423)
24. Mahato RN, Lulf H, Siekman MH, Kersten SP, Bobbert PA, de Jong MP, De Cola L, van der Wiel WG. 2013 Ultrahigh magnetoresistance at room temperature in molecular wires. *Science* **341**, 257–260. (doi:10.1126/science.1237242)
25. Congreve *et al.* DN. 2013 External quantum efficiency above 100% in a singlet-exciton-fission-based organic photovoltaic cell. *Science* **340**, 334–337. (doi:10.1126/science.1232994)
26. Endo A, Sato K, Yoshimura K, Kai T, Kawada A, Miyazaki H, Adachi C. 2011 Efficient up-conversion of triplet excitons into a singlet state and its application for organic light emitting diodes. *Appl. Phys. Lett.* **98**, 083302. (doi:10.1063/1.3558906)
27. Macia F, Wang F, Harmon NJ, Kent AD, Wohlgenannt M, Flatte ME. 2014 Organic magnetoelectroluminescence for room temperature transduction between magnetic and optical information. *Nat. Commun.* **5**, 3609. (doi:10.1038/ncomms4609)
28. Wang F, Macià F, Wohlgenannt M, Kent AD, Flatté ME. 2012 Magnetic fringe-field control of electronic transport in an organic film. *Phys. Rev. X* **2**, 021013. (doi:10.1103/PhysRevX.2.021013)
29. Hellwig O, Berger A, Kortright JB, Fullerton EE. 2007 Domain structure and magnetization reversal of antiferromagnetically coupled perpendicular anisotropy films. *J. Magn. Magn. Mater.* **319**, 13–55. (doi:10.1016/j.jmmm.2007.04.035)
30. Kent AD, Yu J, Rūdiger U, Parkin SSP. 2001 Domain wall resistivity in epitaxial thin film microstructures. *J. Phys. Condens. Matter* **13**, R461–R488. (doi:10.1088/0953-8984/13/25/202)
31. Wohlgenannt M, Flatté ME, Harmon NJ, Wang F, Kent AD, Macià F, Fischer P, Im M-Y. 2013 A new twist on organic spintronics: controlling transport in organic sandwich devices using fringe fields from ferromagnetic films. *Proc. SPIE* **8813**, 88130O. (doi:10.1117/12.2024602)
32. Nguyen TD, Ehrenfreund E, Vardeny ZV. 2012 Spin-polarized light-emitting diode based on an organic bipolar spin valve. *Science* **337**, 204–209. (doi:10.1126/science.1223444)